AIAA JOURNAL
Vol. 34, No. 5, May 1996

Curved Piezoactuator Model for Active Vibration Control of Cylindrical Shells

Venkata R. Sonti*
Automated Analysis Corporation, Peoria, Illinois 61602
and
James D. Jones†
Purdue University, West Lafayette, Indiana 47907-1077

A composite differential equation of motion for a bimorph configured thin curved uniformly polarized piezoactuator pair surface bonded to a cylindrical shell is derived and the approximate analytical expressions for the equivalent forces exerted by the actuator on a cylindrical shell are obtained. The in-phase configuration is studied. The piezoactuators exert x and θ line forces and a uniform pressure load over the patch for in-phase configuration. The in-phase forces show a saturation behavior with increase in thickness.

Nomenclature

a	= radius of the shell
c	= stiffness matrix
$\{D\}$	= 3 × 1 dielectric displacement vector
D_c	= laminated composite bending stiffness
D_p	= flat plate or shell bending stiffness
d_{ij}	= piezoelectric stress constants denoted by the matrix $[d]$
$\{E\}$	= 3 × 1 electric field vector applied to the actuator
F_x, F_θ, F_z	= piezoactuator equivalent forces
$[g]$	= piezoelectric charge constant matrix
H	= Heaviside or step function
h_s	= shell thickness
h_1, h_2	= shell and actuator thickness, respectively, in a composite
$\{K\}$	= bending strain vector
$K_{xx}, K_{x\theta}, K_{\theta\theta}$	= components of the bending strain vector, 1/m
k	= variable denoting the layer number in a laminated composite
L	= axial length of the cylinder
M	= constant denoting the product of free piezoelectric strains, the piezoactuator bending stiffness, and the composite bending stiffness ratios
$M_{xx}, M_{x\theta}, M_{\theta\theta}$	= moment resultants, N-m/m
$N_{xx}, N_{x\theta}, N_{\theta\theta}$	= force resultants, N/m
n	= total number of actuator layers, 1 or 2
$\{Q\}$	= charge vector induced in the piezoelectric material
$\{S\}$	= elastic strain vector, m/m
$S_{xx}, S_{x\theta}, S_{\theta\theta}$	= components of the in-plane strain, m/m
$[s]$	= compliance matrix
$\{T\}$	= stress vector
t	= time variable
u_x, u_θ, u_z	= displacement variables
x, θ, z	= cylindrical coordinates
x_i	= actuator boundaries in the x direction, $i = 1, 2$
Y	= Young's modulus
$\Delta x^0, \Delta\theta^0$	= x and θ direction free piezoelectric strains
δ	= Dirac delta function
$\delta_{si}, \delta_{peki}$	= constants used in defining the composite stiffness, $i = 1, 2, 3$
δ_{tk}, δ_{bk}	= distances of the top and the bottom surface of the kth layer in the composite
$[\epsilon]$	= dielectric permittivity matrix
θ	= coordinate in circular or cylindrical coordinates
μ	= Poisson's ratio
ρ	= material density
ρh	= sum of the product for all of the layers in the composite, $\sum \rho_k h_k$
$[\,]$	= matrix

Subscripts

c	= laminated composite
ij	= effect (stress or strain) produced in the j direction due to an applied action (electric field) in the i direction; elements of a matrix
pe	= piezoactuator
r	= radial component in polar coordinates
s	= cylindrical shell
x	= axial direction in cylindrical coordinates
$xx, \theta\theta, x\theta$	= stress and strain components
z	= transverse or the radial direction in cylindrical coordinates
θ	= related to θ direction
θ_i	= actuator boundaries in the θ direction, $i = 1, 2$
1, 2, 3	= three normal stress or strain directions
4, 5, 6	= three shear (stress or strain) directions

Superscripts

E	= at constant electric field, short circuit
T	= at constant stress, clamped condition
t	= matrix transpose
-1	= inverse of a matrix
$'$	= derivative with respect to the argument
$\cdot, \cdot\cdot$	= derivative of the argument with respect to time

Received Sept. 14, 1994; revision received July 14, 1995; accepted for publication July 14, 1995.

*Senior Project Engineer, Department of Noise and Vibration Analysis, 6516 N University, Apartment 704.

†Professor, School of Mechanical Engineering, 1077 Ray W. Herrick Laboratories.

Introduction

RECENT advances in piezoelectric materials for actuation and sensing of structural motion have generated a strong interest in active structural acoustic control (ASAC). A significant level of analytical and experimental research has been conducted on the use of surface-bonded piezoactuators on a number of actuation and control problems involving beams,[1,2] plates,[3,4] and cylinders.[5–9] Analytical flat models have been developed and used even for cylindrical shells

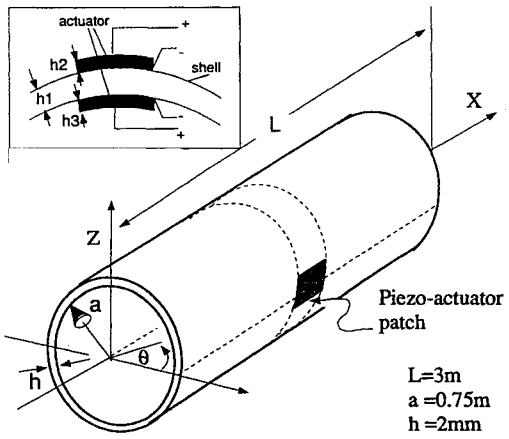

Fig. 1 Cylindrical shell with a surface-bonded piezoactuator.

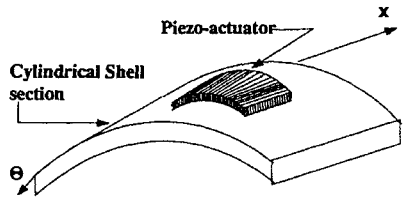

Fig. 2 Schematic of a curved piezoactuator.

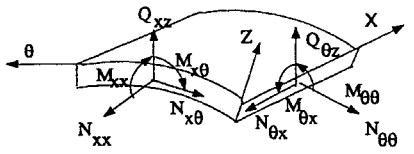

Fig. 3 Free body diagram showing an element of a shell and the force and moment resultants.

with curvature. It is known that curvature causes significant coupling between in-plane and out-of-plane motions and that the magnitude of the piezoactuator force is a function of the substructure properties. Thus, for applications related to active noise and vibration control problems, such as in aircraft, submarines, compressor shells, etc., a piezoactuator model needs to be developed that incorporates the effect of substructure curvature.

In this investigation, a curved actuator model is developed from the composite differential equation of motion for a bimorph piezoactuator patch configuration surface bonded to a thin cylindrical shell (one actuator patch on the inside and one on the outside). Figure 1 shows a schematic of the system. It is assumed that both the actuators are uniformly polarized and are driven in phase. The reason for this is that the in-phase driven configuration (for flat actuator models bonded to cylindrical shell) has in previous studies[6] shown to couple better into lower order shell modes (which make most of the noise) and, thus, cause less spillover into higher order shell modes. Approximate analytical expressions for the equivalent forces exerted by the curved actuator on the cylinder are obtained assuming static conditions. The specific types of equivalent forces (e.g., line forces, pressure forces, etc.) are determined and their amplitude behavior as a function of actuator thickness presented. In a companion paper,[10] the static equivalent force expressions developed here will be used and the validity of the static model studied using wave propagation technique.

Chaudhry et al.[11] have recently presented the same mathematical expressions for equivalent forces of in-phase and out-of-phase driven actuators using Donnell–Mushtari theory.

Cylindrical Coordinate Piezoelectric-Elastic Equations

In this section, various equations required to derive the complete composite cylinder/actuator system equations are presented. The dynamic cylindrical shell equations are shown and the electromechanical equations describing the dynamic behavior of a curved piezoactuator are derived. The piezoactuator has the shape of a section cut from a cylindrical shell surface and, thus, is curved in the θ direction and is straight in the x direction (see Figs. 1 and 2). The complete system involves layers of piezoactuators and the cylindrical shell substructure.

The equations of motion for a thin homogenous in vacuo circular cylindrical shell using Love's theory[12] of thin shells are given by

$$\frac{\partial N_{xx}}{\partial x} + \frac{1}{a}\frac{\partial N_{x\theta}}{\partial \theta} - \rho_s h_s \frac{\partial^2 u_x}{\partial t^2} = 0 \tag{1}$$

$$\frac{\partial N_{x\theta}}{\partial x} + \frac{1}{a}\frac{\partial N_{\theta\theta}}{\partial \theta} + \frac{1}{a}\left(\frac{\partial M_{x\theta}}{\partial x} + \frac{1}{a}\frac{\partial M_{\theta\theta}}{\partial \theta}\right) - \rho_s h_s \frac{\partial^2 u_\theta}{\partial t^2} = 0 \tag{2}$$

$$\frac{\partial^2 M_{xx}}{\partial x^2} + \frac{2}{a}\frac{\partial^2 M_{x\theta}}{\partial x \partial \theta} + \frac{1}{a^2}\frac{\partial^2 M_{\theta\theta}}{\partial \theta^2} - \frac{N_{\theta\theta}}{a} - \rho_s h_s \frac{\partial^2 u_z}{\partial t^2} = 0 \tag{3}$$

where N_{xx} and M_{xx} are the force and moment resultants in the x direction, $N_{x\theta}$ and $M_{x\theta}$ the shear force and twisting moment resultants, and $N_{\theta\theta}$ and $M_{\theta\theta}$ the force and the moment resultants in the θ direction, respectively (see Fig. 3). Also ρ_s is the density of the shell. The variables u_x, u_θ, and u_z are the axial, torsional, and transverse displacements measured at the neutral surface. In deriving these equations transverse shear strains and rotational inertia are neglected.[13]

The force and moment resultants are given by the following equations:

$$\begin{bmatrix} N_{xx} \\ N_{\theta\theta} \\ N_{x\theta} \end{bmatrix} = \int_{-\frac{h_x}{2}}^{\frac{h_x}{2}} \begin{bmatrix} T_{xx} \\ T_{\theta\theta} \\ T_{x\theta} \end{bmatrix} dz, \qquad \begin{bmatrix} M_{xx} \\ M_{\theta\theta} \\ M_{x\theta} \end{bmatrix} = \int_{-\frac{h_x}{2}}^{\frac{h_x}{2}} \begin{bmatrix} T_{xx} \\ T_{\theta\theta} \\ T_{x\theta} \end{bmatrix} z\, dz \tag{4}$$

where T_{xx}, $T_{\theta\theta}$, and $T_{x\theta}$ are the three stress vector components representing the normal stresses in the x and θ directions and the shear stress in the x–θ plane, respectively. These stresses are obtained from the linear stress-strain relations (Hooke's law). For a nonpiezoelectric material these stress-strain relations involve only the stiffness matrix. Because the elastic and the piezoelectric properties are coupled for a piezoelectric material, however, the stress-strain relations also involve the piezoelectric properties. The stress resultants for the individual layers (actuators and shell) in the laminate need to be obtained, summed, and then substituted in Eqs. (1–3) to develop the composite dynamic equations (this is done later).

The simplified linear electromechanical equations for a piezoelectric material in plane stress are given by[4]

$$\begin{aligned} S_1 &= s_{11}^E T_1 + s_{12}^E T_2 + d_{31} E_3 \\ S_2 &= s_{11}^E T_2 + s_{12}^E T_1 + d_{31} E_3 \\ S_6 &= s_{66} T_6 \\ D_3 &= \epsilon_{33} E_3 + d_{31}(T_1 + T_2) \end{aligned} \tag{5}$$

The first three equations of Eq. (5) are also known as the actuator equations because they relate the applied electric field to the strain developed in the material. The last equation is known as the sensor equation that relates the charge developed in the piezoelectric material due to the induced stresses or strains. Next, the actuator equations in Eq. (5) will be used to derive the expressions for in-plane stresses generated when the curved [see Figs. 1 (inset) and 2] piezoelectric actuators are subjected to an in-phase electric field in the transverse z direction. Note that both piezoactuators undergo the same deformation when an in-phase voltage is applied. Thus, the substructure is mostly in pure extension or pure compression (see Fig. 4).

The strain vector $\{S\}$ in Eqs. (5) (with elements S_1 or S_{xx}, S_2 or $S_{\theta\theta}$, and S_6 or $S_{x\theta}$) may be written as

$$\{S\} = \{S^0\} + z\{K\} \tag{6}$$

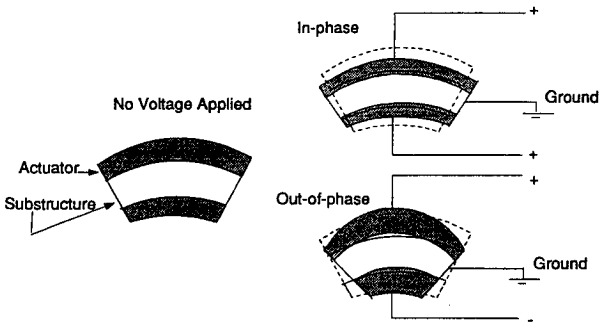

Fig. 4 In-phase and out-of-phase configurations of piezoactuator/substructure system.

where $\{S^0\}$ and $\{K\}$ are the membrane and bending strain vectors, respectively. The individual components of $\{S^0\}$ and $\{K\}$ in cylindrical coordinates are given by

$$S_{xx} = \frac{\partial u_x}{\partial x} \qquad S_{\theta\theta} = \frac{1}{a}\frac{\partial u_\theta}{\partial \theta} + \frac{u_z}{a}$$

$$S_{x\theta} = \frac{1}{a}\frac{\partial u_x}{\partial \theta} + \frac{\partial u_\theta}{\partial x} \qquad K_{xx} = -\frac{\partial^2 u_z}{\partial x^2} \tag{7}$$

$$K_{\theta\theta} = \frac{1}{a^2}\left(\frac{\partial u_\theta}{\partial \theta} - \frac{\partial^2 u_z}{\partial \theta^2}\right) \qquad K_{x\theta} = \frac{1}{a}\frac{\partial u_\theta}{\partial x} - \frac{2\partial^2 u_z}{a\partial x \partial \theta}$$

where the subscripts xx and $\theta\theta$ stand for normal strains in x and θ directions, respectively. The subscript $x\theta$ stands for the shear strain. The preceding strain-displacement relations imply that z/a is neglected in comparison to unity.

The actuator equations in compact vector notation are[4]

$$\{S\} = [s^E]\{T\} + [d]^t\{E\} \tag{8}$$

where $[s^E]$ is the compliance matrix with $\{E\} = 0$. Next, Eq. (8) is rewritten with stress as the dependent variable since stress resultants are needed for substitution in Eqs. (1–3):

$$\{T\} = [c^E]\{S\} - [e]\{E\} \tag{9}$$

where $[c^E]$ is the stiffness matrix. Here $[e]$ is $[s^E]^{-1}[d]^t$ and the product $[e]\{E\}$ defines stress related to the free strains of the piezoactuator Δ_x^0 and Δ_θ^0 (i.e., the strains obtained in the x and the θ directions in the piezoactuator under free stress conditions when an electric field is applied in the z direction). If the strain vector $\{S\}$ is set to zero, a clamped condition is obtained at the boundaries. The stress $\{T\}$ then turns out to be $-[e]\{E\}$, a negative quantity implying compression. This is logical because an applied positive electric field tends to extend the material and the imposed clamped strain boundary conditions prevent this. Analogously, if the stress vector $\{T\}$ is set to zero, thus imposing a free boundary condition, the strain vector $\{S\}$ becomes $[d]^t\{E\}$, which is the expression for free piezoactuator strains [this is clearer in Eqs. (5)]. Thus, the free strains Δ_x^0 and Δ_θ^0 are both equal to $d_{31}E_3$.

The presence of initial curvature and the strain in the third direction due to d_{33} [the constant relating the strain in the z (or third) direction to the applied field in the z (or third) direction] causes a change in the curvature of the actuator in the θ direction in its free state when E_3 is applied. This is due to the initial difference in the length of the top and the bottom surfaces of the actuator that causes a further differential expansion, thus causing a change in curvature. The thermal expansion analog has been discussed by Boley and Weiner[14] for curved beams where it is also stated that for very small thickness to radius ratios (such as the curved actuator) this change in curvature is negligible. Hence, in the current analysis, it is assumed that the free strains of the actuator involve no change in curvature. This is the reason for both the x and θ free strain expressions being equal.

All of the equations needed to derive the final composite shell/actuator dynamic equations have been presented. In the following sections, the composite equations are derived and from them the piezoactuator equivalent forces obtained.

Derivation of Piezoactuator Equivalent Forces

In this section, the composite differential equation of motion for a circular cylindrical shell with surface-bonded piezoactuators is derived using the equations presented in the preceding section. The configuration involves two actuators bonded to the shell, one on the inside and one on the outside (see Fig. 1). Once this differential equation is obtained, equivalent forcing functions in all three directions (x, θ, and z) are derived after making several simplifying approximations.

The first assumption involved in this derivation is that the actuators and the substructure are perfectly bonded, which results in the absence of interfacial shear and the continuity of normal strain across the interface. It is also assumed that Poisson's ratios of the actuator and the shell material are equal (i.e., $\mu_{pe} = \mu_s$). Piezoceramics typically have a Poisson's ratio of 0.29 and metallic shell substructures normally have 0.31, which makes the assumption reasonable. Thus, Poisson's ratio of the shell (0.31) will be assumed for the actuator also. Further, it is assumed that Young's moduli, the thicknesses, and Poisson's ratios of the layers involved do not vary with respect to any coordinate within the actuator patch boundary. This and the earlier assumption are important as they facilitate some convenient factorizations. Next, the static mass effect of the actuator is assumed negligible compared to the total shell/actuator system. The composite is assumed thin in relation to the shell radius, and so Love's thin shell theory is still applicable.

Equations (4) define the force and the moment resultants for a differential element of a single layer (or laminate) of a laminated composite material, piezoelectric or nonpiezoelectric [this depends on whether the $[d]$ matrix in Eq. (8) is nonzero or not]. To obtain the resultants, the stresses are computed from Eq. (9) where the matrix $\{e\}$ is set to zero for a nonpiezoelectric layer. The resultants for a differential element of a laminated composite (consisting of multiple layers) may be obtained by summing up the resultants from the individual layers in the following manner:

$$\begin{bmatrix} N_{xx} \\ N_{\theta\theta} \\ N_{x\theta} \end{bmatrix} = \sum_{k=1}^{k=N} \int_{\delta_{k-1}}^{\delta_k} \begin{bmatrix} T_{xxk} \\ T_{\theta\theta k} \\ T_{x\theta k} \end{bmatrix} dz$$

$$\begin{bmatrix} M_{xx} \\ M_{\theta\theta} \\ M_{x\theta} \end{bmatrix} = \sum_{k=1}^{k=N} \int_{\delta_{k-1}}^{\delta_k} \begin{bmatrix} T_{xxk} \\ T_{\theta\theta k} \\ T_{x\theta k} \end{bmatrix} z\, dz \tag{10}$$

where k denotes the kth layer and δ_k and δ_{k-1} are the distances from the top and the bottom surfaces of the kth layer to the neutral surface. These resultants in turn are substituted into Eqs. (1–3) in order to obtain the composite differential equation.

To facilitate the explicit derivation of the composite differential equation and for the purpose of clarity in presentation, the following parameters that arise as a result of the integrations in Eqs. (10) are defined:

$$\delta_{s1} = \frac{Y_s h_1}{1-\mu^2} \qquad \delta_{s2} = \frac{Y_s}{1-\mu^2}\frac{\left(\delta_{t1}^2 - \delta_{b1}^2\right)}{2}$$

$$\delta_{s3} = \frac{Y_s}{1-\mu^2}\frac{\left(\delta_{t1}^3 - \delta_{b1}^3\right)}{3} \tag{11}$$

$$\delta_{pek1} = \frac{Y_{pe} h_k}{1-\mu^2} \qquad \delta_{pek2} = \frac{Y_{pe}}{1-\mu^2}\frac{\left(\delta_{tk}^2 - \delta_{bk}^2\right)}{2}$$

$$\delta_{pek3} = \frac{Y_{pe}}{1-\mu^2}\frac{\left(\delta_{tk}^3 - \delta_{bk}^3\right)}{3} \tag{12}$$

where the constants δ_{s1}, δ_{s2}, and δ_{s3} in Eq. (11) are related to the cylindrical substructure and δ_{pek1}, δ_{pek1}, and δ_{pek1} in Eqs. (12) to the piezoactuator layers. The constants Y_s and Y_{pe} are Young's moduli of the shell material and the piezoceramic, respectively. The variables δ_{tk} and δ_{bk} are the distances from the top and the bottom surfaces of a laminate to the neutral axis of the composite. The subscript $k = 1$ represents the substructure (i.e., the cylindrical shell) and $k = 2$

or 3 represents the piezoactuator layer bonded on the outside or the inside of the shell, respectively. Thus, h_2 and h_3 are the actuator thicknesses. In this entire study h_2 is assumed equal to h_3. The variable δ_{pek} is either the outer piezoactuator or the inner one depending on whether $k = 2$ or 3.

As already mentioned, the individual force and moment resultants of each of the laminates need to be added to obtain the resultants for the entire lamina [Eqs. (10)]. The resultants of the individual layers are obtained after the integration and before the summation. The following define explicitly the individual force and moment resultants for each of the three layers (one shell and two piezoactuators). It should be noted that both actuators are driven in phase. Thus, their free strains have the same algebraic sign. The resultants are given by

$$
\begin{aligned}
N_{xx\,\text{cylinder}} &= \delta_{s1}(S_{xx} + \mu S_{\theta\theta}) + \delta_{s2}(K_{xx} + \mu K_{\theta\theta}) \\
N_{xx\,\text{pzt}\,k=2,3} &= \delta_{pek1}(S_{xx} + \mu S_{\theta\theta}) + \delta_{pek2}(K_{xx} + \mu K_{\theta\theta}) \\
&\quad - \delta_{pek1}(\Delta x^0 + \mu \Delta\theta^0) \\
N_{\theta\theta\,\text{cylinder}} &= \delta_{s1}(S_{\theta\theta} + \mu S_{xx}) + \delta_{s2}(K_{\theta\theta} + \mu K_{xx}) \\
N_{\theta\theta\,\text{pzt}\,k=2,3} &= \delta_{pek1}(S_{\theta\theta} + \mu S_{xx}) + \delta_{pek2}(K_{\theta\theta} + \mu K_{xx}) \\
&\quad - \delta_{pek1}(\Delta\theta^0 + \mu \Delta x^0) \\
N_{x\theta\,\text{cylinder}} &= \delta_{s1}[(1+\mu)/2]S^0_{x\theta} + \delta_{s2}[(1+\mu)/2]k^0_{x\theta} \\
N_{x\theta\,\text{pzt}\,k=2,3} &= \delta_{pek1}[(1+\mu)/2]S^0_{x\theta} + \delta_{pek2}[(1+\mu)/2]k^0_{x\theta} \\
M_{xx\,\text{cylinder}} &= \delta_{s2}(S_{xx} + \mu S_{\theta\theta}) + \delta_{s3}(K_{xx} + \mu K_{\theta\theta}) \\
M_{xx\,\text{pzt}\,k=2,3} &= \delta_{pek2}(S_{xx} + \mu S_{\theta\theta}) + \delta_{pek3}(K_{xx} + \mu K_{\theta\theta}) \\
&\quad - \delta_{pek2}(\Delta x^0 + \mu \Delta\theta^0) \\
M_{\theta\theta\,\text{cylinder}} &= \delta_{s2}(S_{\theta\theta} + \mu S_{xx}) + \delta_{s3}(K_{\theta\theta} + \mu K_{xx}) \\
M_{\theta\theta\,\text{pzt}\,k=2,3} &= \delta_{pek2}(S_{\theta\theta} + \mu S_{xx}) + \delta_{pek3}(K_{\theta\theta} + \mu K_{xx}) \\
&\quad - \delta_{pek2}(\Delta\theta^0 + \mu \Delta x^0) \\
M_{x\theta\,\text{cylinder}} &= \delta_{s2}[(1+\mu)/2]S^0_{x\theta} + \delta_{s3}[(1+\mu)/2]k^0_{x\theta} \\
M_{x\theta\,\text{pzt}\,k=2,3} &= \delta_{pek2}[(1+\mu)/2]S^0_{x\theta} + \delta_{pek3}[(1+\mu)/2]k^0_{x\theta}
\end{aligned}
\tag{13}
$$

where Δx^0 and $\Delta\theta^0$ are given in Eq. (5).

Substituting Eqs. (13) into Eqs. (1–3) and using Eqs. (11) and (12), the three differential equations (x, θ, z) for the composite differential element are given by

$$
\left(\frac{Y_s}{1-\mu^2}h_1 + 2*\frac{Y_{pe}}{1-\mu^2}h_2\right)\left(\frac{\partial}{\partial x}(S_{xx} + \mu S_{\theta\theta}) + \frac{1+\mu}{2a}\frac{\partial}{\partial\theta}S_{x\theta}\right)
$$

$$
- \rho h\ddot{u}_x = 2\frac{Y_{pe}}{1-\mu^2}h_2\frac{\partial}{\partial x}\left(\Delta^0_x + \mu\Delta^0_\theta\right) \tag{14}
$$

$$
\left(\frac{Y_s}{1-\mu^2}h_1 + 2*\frac{Y_{pe}}{1-\mu^2}h_2\right)\left[\frac{1}{a}\frac{\partial}{\partial\theta}(S_{\theta\theta} + \mu S_{xx}) + \left(\frac{1-\mu}{2}\right)\frac{\partial}{\partial x}S_{x\theta}\right] + \left[\frac{Y_s}{1-\mu^2}\left(\frac{\delta^3_{t1} - \delta^3_{b1}}{3}\right) + 2*\frac{Y_{pe}}{1-\mu^2}\left(\frac{\delta^3_{t2} - \delta^3_{b2}}{3}\right)\right]\left[\frac{1}{a^2}\frac{\partial}{\partial\theta}(K_{\theta\theta} + \mu K_{xx}) + \frac{1+\mu}{2a}\frac{\partial}{\partial x}K_{x\theta}\right] - \rho h\ddot{u}_\theta = 2\frac{1}{a}\frac{Y_{pe}}{1-\mu^2}h_2\frac{\partial}{\partial\theta}\left(\Delta^0_\theta + \mu\Delta^0_x\right) \tag{15}
$$

$$
\left[\frac{Y_s}{1-\mu^2}\left(\frac{\delta^3_{t1} - \delta^3_{b1}}{3}\right) + 2*\frac{Y_{pe}}{1-\mu^2}\left(\frac{\delta^3_{t2} - \delta^3_{b2}}{3}\right)\right] \times \left[\frac{\partial^2}{\partial x^2}(K_{xx} + \mu K_{\theta\theta}) + \frac{2}{a}\left(\frac{1-\mu}{2}\right)\frac{\partial^2}{\partial x\partial\theta}K_{x\theta} + \frac{1}{a^2}\frac{\partial^2}{\partial\theta^2}(K_{\theta\theta} + \mu K_{xx})\right] - \frac{1}{a}\left(\frac{Y_s}{1-\mu^2}h_1 + 2*\frac{Y_{pe}}{1-\mu^2}h_2\right) \times (S_{\theta\theta} + \mu S_{xx}) - \rho h\ddot{u}_z = -2\frac{1}{a}\frac{Y_{pe}}{1-\mu^2}h_2\left(\Delta^0_\theta + \mu\Delta^0_x\right) \tag{16}
$$

where the product ρh is given by $\sum \rho_k h_k$, where k is the number of the layer. Equations (14–16) are defined only in the composite part of the system where the piezoactuators are surface bonded to the shell. They include the stiffness and inertial properties of both the shell and the actuators within the composite region. Thus, these equations do not represent the total system (the entire shell and the piezoactuator). In the following, the effects of the actuator dynamics are neglected due to its relative small size, and approximate expressions are obtained for the equivalent forces exerted on cylindrical shell.

The effect of a small piezoactuator on a relatively large homogenous cylinder may be visualized as a combination of four elements: a static stiffness (analogous to static force applied to a spring to induce a unit displacement), a dynamic stiffness, a static mass, and a dynamic mass. The two dynamic components model the natural frequencies and related effects and are not easy to represent mathematically due to the distributed nature of the piezoactuator. Their effect may only be estimated. The static (gravitational) mass effect is assumed negligible due to the smallness of the actuator.

Thus, initially the static stiffness of the actuators is included, the inertial term is omitted from the equations, and the static equilibrium of the actuators/shell system with a transverse static voltage applied to the piezoactuators is studied. The applied in-phase voltage causes the actuators to strain, which is transmitted to the shell. Then an estimate of the equivalent forces exerted on the shell substructure alone is obtained. This procedure is presented one equation at a time in the following sections. In a companion paper[10] shell responses with and without the actuator dynamic effects are compared in order to verify the static assumptions of the curved actuator model.

x Equation of Motion

The equivalent force on the right side of Eq. (14) is an x-direction line force (see Fig. 7b). The reason why the expression represents a line force will be discussed later. The entire composite differential element is in equilibrium with this force. Thus, there is a resultant line force acting on the cylindrical substructure alone (since it is also in equilibrium). The force must be equal to the shell stiffness term arising out of its deformation, which is given by

$$
\frac{Y_s}{1-\mu^2}h_1\left(\frac{\partial}{\partial x}(S_{xx} + \mu S_{\theta\theta}) + \frac{1+\mu}{2a}\frac{\partial}{\partial\theta}S_{x\theta}\right) \tag{17}
$$

The term may be obtained by multiplying Eq. (14) by the following ratio:

$$
\left(\frac{Y_s}{1-\mu^2}h_1\right)\Big/\left(\frac{Y_s}{1-\mu^2}h_1 + 2*\frac{Y_{pe}}{1-\mu^2}h_2\right) \tag{18}
$$

which is the ratio of the cylinder homogenous membrane stiffness to the composite actuator/cylinder membrane stiffness. Finally, the x-direction static cylindrical shell equation is obtained as

$$
\begin{aligned}
&\frac{Y_s}{1-\mu^2}h_1\left(\frac{\partial}{\partial x}(S_{xx} + \mu S_{\theta\theta}) + \frac{1+\mu}{2a}\frac{\partial}{\partial\theta}S_{x\theta}\right) \\
&\quad = 2\left[\left(\frac{Y_s}{1-\mu^2}h_1\right)\Big/\left(\frac{Y_s}{1-\mu^2}h_1 + 2*\frac{Y_{pe}}{1-\mu^2}h_2\right)\right] \\
&\quad\quad \times \left(\frac{Y_{pe}}{1-\mu^2}\right)h_2\frac{\partial}{\partial x}\left(\Delta^0_x + \mu\Delta^0_\theta\right)
\end{aligned}
\tag{19}
$$

where the right side represents the equivalent force exerted on the cylindrical substructure alone. Equation (19) was derived using static assumptions. Next, the forcing term on the right side is incorporated into the dynamic shell equation involving only the shell inertial term. This implies that the inertial effects of the actuator material are negligible. Equation (19) then becomes

$$\frac{Y_s h_1}{1-\mu^2}\left(\frac{\partial}{\partial x}(S_{xx}+\mu S_{\theta\theta})+\frac{1+\mu}{2a}\frac{\partial}{\partial\theta}S_{x\theta}\right)-\rho_1 h_1 \ddot{u}_x$$
$$=2\left[\left(\frac{Y_s}{1-\mu^2}h_1\right)\Big/\left(\frac{Y_s}{1-\mu^2}h_1+2*\frac{Y_{pe}}{1-\mu^2}h_2\right)\right]$$
$$\times\frac{Y_{pe}}{1-\mu^2}h_2\frac{\partial}{\partial x}\left(\Delta_x^0+\mu\Delta_\theta^0\right) \tag{20}$$

In Eq. (14), the expression on the right side represents the blocked force exerted by the piezoactuator, i.e., the force a piezoactuator exerts on its boundaries when it is totally clamped in the x direction. On the left side, the product of the piezoactuator membrane stiffness and the strain terms is the force required to extend the piezoactuator. Hence, the difference of these two terms is the force that extends the substructure.

The actual mechanism of strain transfer occurs through the interfacial stress. In this scheme, the interfacial stress does not appear in the picture since a perfect bond has been assumed. In actuality, the interfacial stress will not appear even if it was not neglected in the model since the derivation deals with the stress resultants (which are integrations of stresses over the thickness). It has been shown that in the presence of a bonding layer that is so very thin that it approaches a perfect bond, the interfacial stresses concentrate at the ends of the actuator.[15,16] This in turn gives rise to transverse shear stresses in the substructure at the lateral faces (boundaries) of the actuator. Because of the in-phase actuation, the resultants due to these transverse stresses are also zero (since they are antisymmetric with respect to the neutral axis). The current simplified model deals with the composite as a whole and, hence, cannot accommodate the transverse shear stresses in the individual layers. But for one-dimensional and two-dimensional flat actuator cases and for thin piezoactuators this integrated approach has given reasonably accurate results.[3,17] It is assumed that this argument applies when curvature is included for two-dimensional thin actuators that are significantly smaller than the substructure.

Lastly, the state of stress assumed results in normal stresses at the free edges of the actuator. The actual stress distribution will have zero normal stresses at the free edges (since they are traction free) but the same resultant. But Liang and Rogers[18] have shown that the stress distribution in a distributed actuator is not influenced by the free edge beyond four actuator thicknesses from the boundary. Since typical actuators have a thickness dimension of 0.01 in. and lateral dimensions of 1×2 in., the assumed state of stress should be reasonable for most of the actuator patch and the obtained approximate equivalent force expressions should be acceptable.

θ Equation of Motion

Equation (15) is the θ equation of motion that is quite similar to the x equation with one exception. The transverse shear force has small contributions in the θ direction due to curvature (Fig. 5a). This contribution vanishes as the radius increases. Also, the forcing term on the right side is again an in-plane line force in the θ direction (see Fig. 7c). Thus, for in-phase excitation, the piezoactuator exerts an x-direction line force, a θ-direction line force, and a third equivalent force in the transverse direction [Eq. (16)] that turns out to be a

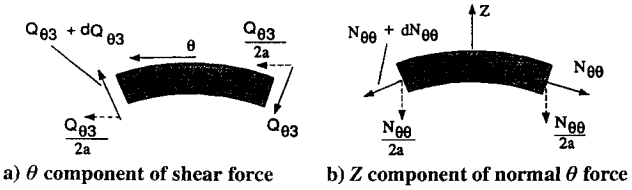

a) θ component of shear force b) Z component of normal θ force

Fig. 5 Force coupling in θ and Z directions due to curvature.

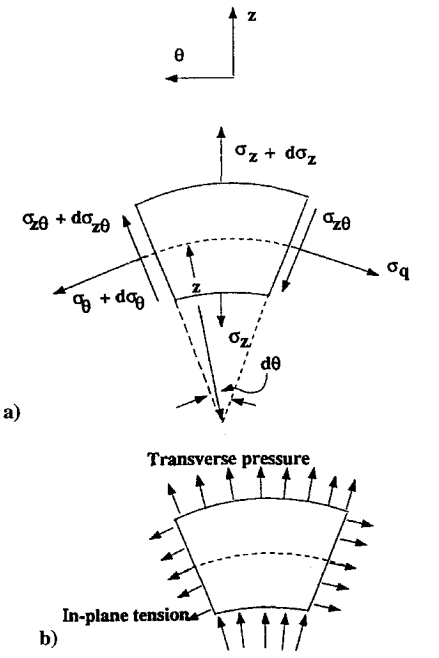

Fig. 6 Two-dimensional differential element in cylindrical coordinates.

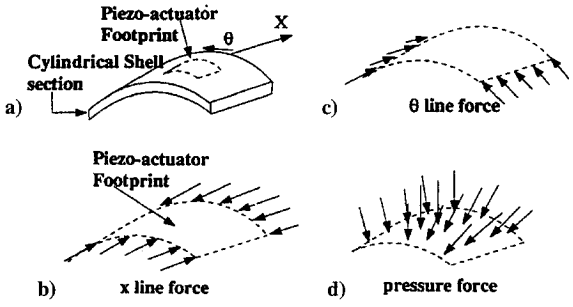

Fig. 7 Schematic representation of the equivalent forces.

uniform pressure force over the actuator surface (see Fig. 7d). The x line force may be studied independently from the other two equivalent forces. The transverse pressure force, however, arises due to the θ line force as shown in Fig. 5b. Thus, both the forces need to be considered simultaneously for analysis.

The equations of static equilibrium of a differential element in cylindrical coordinates are given by

$$\frac{\partial\sigma_z}{\partial z}+\frac{1}{z}\frac{\partial\sigma_{z\theta}}{\partial\theta}+\frac{\sigma_z-\sigma_\theta}{z}=0$$
$$\frac{1}{z}\frac{\partial\sigma_\theta}{\partial\theta}+\frac{\partial\sigma_{z\theta}}{\partial z}+\frac{2\sigma_{z\theta}}{z}=0 \tag{21}$$

where z is the radial coordinate and σ_z and $\sigma_{z\theta}$ are the radial and the transverse shear stresses. The component σ_θ is the usual tangential stress (see Fig. 6).

From Love's shell theory, the variation of σ_z with z is negligible for a thin shell. If the element is subjected to pure extension in the tangential direction (θ line force) and pure radial stresses (transverse pressure) on the inner and outer radius (as shown in Fig. 6b), then it may be seen that σ_θ is also independent of z (uniform in-plane tension). Thus, $\sigma_{z\theta}$ from the first of Eqs. (21) is independent of z. And if neither the outer nor the inner surfaces are subjected to shear forces (consistent with our assumption of no interfacial shear), $\sigma_{z\theta}$ is zero at the boundaries. This implies that the shear stress is zero all through the thickness. Thus, in Eq. (15) the resistance to the in-plane forces and transverse pressure force is purely through membrane stiffness at the section where the in-plane forces are applied. Hence, the θ in-plane shell stiffness should give an estimate of the θ line force.

Equation (15) (without the inertial term) is multiplied by the same ratio as before [Eq. (18)] and this results in

$$\frac{Y_s}{1-\mu^2}h_1\left[\frac{1}{a}\frac{\partial}{\partial\theta}(S_{\theta\theta}+\mu S_{xx})+\frac{1+\mu}{2}\frac{\partial}{\partial x}S_{x\theta}\right]$$
$$+\left[\left(\frac{Y_s}{1-\mu^2}h_1\right)\Big/\left(\frac{Y_s}{1-\mu^2}h_1+2*\frac{Y_{pe}}{1-\mu^2}h_2\right)\right]$$
$$\times\left[\frac{Y_s}{1-\mu^2}\left(\frac{\delta_{t1}^3-\delta_{b1}^3}{3}\right)+2*\frac{Y_{pe}}{1-\mu^2}\left(\frac{\delta_{t2}^3-\delta_{b2}^3}{3}\right)\right]$$
$$\times\left[\frac{1}{a^2}\frac{\partial}{\partial\theta}(K_{\theta\theta}+\mu K_{xx})+\frac{1+\mu}{2a}\frac{\partial}{\partial x}K_{x\theta}\right]$$
$$=2\left[\left(\frac{Y_s}{1-\mu^2}h_1\right)\Big/\left(\frac{Y_s}{1-\mu^2}h_1+2*\frac{Y_{pe}}{1-\mu^2}h_2\right)\right]$$
$$\times\frac{1}{a}\frac{Y_{pe}}{1-\mu^2}h_2\frac{\partial}{\partial\theta}\left(\Delta_\theta^0+\mu\Delta_x^0\right) \tag{22}$$

where the first term on the left is the in-plane stiffness term.

In the case of the x equation, the actual homogenous shell equation was obtained but in the case of the θ equation, the curvature introduces shear force terms. But as discussed earlier, in this integrated scheme the shear stress resultant will be zero at the section where the in-plane force is applied. Thus, the force estimate can be made using the membrane stiffness. The right-side expressions represent the equivalent forces on the shell in the θ direction. Substituting them in the original θ equation of the shell (after including the inertial term) the following forced equation is obtained:

$$\frac{Y_s}{1-\mu^2}h_1\left[\frac{1}{a}\frac{\partial}{\partial\theta}(S_{\theta\theta}+\mu S_{xx})+\frac{1+\mu}{2}\frac{\partial}{\partial x}S_{x\theta}\right]$$
$$+\frac{Y_s}{1-\mu^2}h_1^3\left[\frac{1}{a^2}\frac{\partial}{\partial\theta}(K_{\theta\theta}+\mu K_{xx})+\frac{1+\mu}{2a}\frac{\partial}{\partial x}K_{x\theta}\right]-\rho_1h_1\ddot{u}_\theta$$
$$=2\left[\left(\frac{Y_s}{1-\mu^2}h_1\right)\Big/\left(\frac{Y_s}{1-\mu^2}h_1+2*\frac{Y_{pe}}{1-\mu^2}h_2\right)\right]$$
$$\times\frac{1}{a}\frac{Y_{pe}}{1-\mu^2}h_2\frac{\partial}{\partial\theta}\left(\Delta_\theta^0+\mu\Delta_x^0\right) \tag{23}$$

The forcing term on the right side is the equivalent forcing function in the θ direction acting on the shell alone. As shown in Fig. 7c it is an in-plane line force in the θ direction for a uniformly polarized actuator arising due to the in-plane normal stress resultant ($N_{\theta\theta}$) of the piezoactuators exerted when the actuators are driven in-phase.

z Equation of Motion

In Eq. (16), which is the transverse equation of motion, the forcing term on the right is a transverse pressure. This pressure load is exerted in order to balance the transverse component of the θ line forces. In the absence of this balancing pressure load, the substructure would experience a rigid-body force that is impossible. Hence, for a small piezoactuator pair the expression for the equivalent pressure load may be obtained by a simple force balance involving the transverse components of the θ line force (see Fig. 8).

The amplitude of the pressure force is finally given by

$$2\left[\left(\frac{Y_s}{1-\mu^2}h_1\right)\Big/\left(\frac{Y_s}{1-\mu^2}h_1+2*\frac{Y_{pe}}{1-\mu^2}h_2\right)\right]$$
$$\times\frac{1}{a}\frac{Y_{pe}}{1-\mu^2}h_2\left(\Delta_\theta^0+\mu\Delta_x^0\right) \tag{24}$$

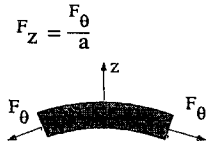

Fig. 8 Pressure load balances in plane θ line force.

The final z equation with the inertial term included is given by

$$\frac{Y_s}{1-\mu^2}\frac{h_1^3}{12}\left[\frac{\partial^2}{\partial x^2}(K_{xx}+\mu K_{\theta\theta})+\frac{2}{a}\frac{1+\mu}{2}\frac{\partial^2}{\partial x\partial\theta}K_{x\theta}\right.$$
$$\left.+\frac{1}{a^2}\frac{\partial^2}{\partial\theta^2}(K_{\theta\theta}+\mu K_{xx})\right]-\frac{1}{a}\frac{Y_s}{1-\mu^2}h_1(S_{\theta\theta}+\mu S_{xx})-\rho_1h_1\ddot{u}_z$$
$$=-2\left[\left(\frac{Y_s}{1-\mu^2}h_1\right)\Big/\left(\frac{Y_s}{1-\mu^2}h_1+2*\frac{Y_{pe}}{1-\mu^2}h_2\right)\right]$$
$$\times\frac{1}{a}\frac{Y_{pe}}{1-\mu^2}h_2\left(\Delta_\theta^0+\mu\Delta_x^0\right) \tag{25}$$

The forcing term on the right is the equivalent force in the z direction. For uniformly polarized actuators this represents a uniform pressure over the patch area (Fig. 7d).

The equivalent forces exerted by two uniformly polarized in-phase driven small curved piezoactuators surface bonded (inside and outside) to a cylindrical shell surface have been derived. Only the two-sided actuator configuration has been presented so that the in-plane extension behavior can be separated from bending behavior with reasonable accuracy. The one-sided case is far more complicated because of the coupling between extension and bending (and shear). Modeling will require ascertaining the relative levels of extension and bending based on shell aspect ratio and excitation frequency. The problem becomes very strongly case dependent and cannot be easily generalized.

The nature of equivalent forces developed in this paper is yet unexplained. In the following sections, the explanation is given and the amplitude variation of these forces as a function of actuator thickness is presented.

Type and Amplitude Variation of Equivalent Forces

Types of Equivalent Forces

In the preceding section, the equivalent forces exerted by piezoactuators on the shell surface were derived. The equivalent forces are

$$F_x=2\left[\left(\frac{Y_s}{1-\mu^2}h_1\right)\Big/\left(\frac{Y_s}{1-\mu^2}h_1+2*\frac{Y_{pe}}{1-\mu^2}h_2\right)\right]$$
$$\times\frac{Y_{pe}}{1-\mu^2}h_2\frac{\partial}{\partial x}\left(\Delta_x^0+\mu\Delta_\theta^0\right)$$
$$F_\theta=2\left[\left(\frac{Y_s}{1-\mu^2}h_1\right)\Big/\left(\frac{Y_s}{1-\mu^2}h_1+2*\frac{Y_{pe}}{1-\mu^2}h_2\right)\right] \tag{26}$$
$$\times\frac{1}{a}\frac{Y_{pe}}{1-\mu^2}h_2\frac{\partial}{\partial\theta}\left(\Delta_\theta^0+\mu\Delta_x^0\right)$$
$$F_z=2\left[\left(\frac{Y_s}{1-\mu^2}h_1\right)\Big/\left(\frac{Y_s}{1-\mu^2}h_1+2*\frac{Y_{pe}}{1-\mu^2}h_2\right)\right]$$
$$\times\frac{1}{a}\frac{Y_{pe}}{1-\mu^2}h_2\left(\Delta_\theta^0+\mu\Delta_x^0\right)$$

where F_x is an equivalent force in the in-plane x direction, F_θ in the in-plane θ direction, and F_z in the transverse z direction. The specific type of the equivalent force (line force or pressure force) was mentioned in the preceding sections, but the reason was not discussed. This section focuses on the type of these forces and also presents the variation of the amplitudes of these forces with the thickness of the actuator.

The free strain variables (Δ_x^0, Δ_θ^0) are defined only within the actuator boundaries. Thus, the free strain variables should include the information regarding the spatial extent of the actuator. This can be done using the Heaviside functions, also known as the unit step functions, as follows:

$$M[H(x-x_1)-H(x-x_2)][H(\theta-\theta_1)-H(\theta-\theta_2)] \tag{27}$$

where M is the constant consisting of the free strains and $H(x)$ is the Heaviside function. The variables x_1, x_2, θ_1, and θ_2 define

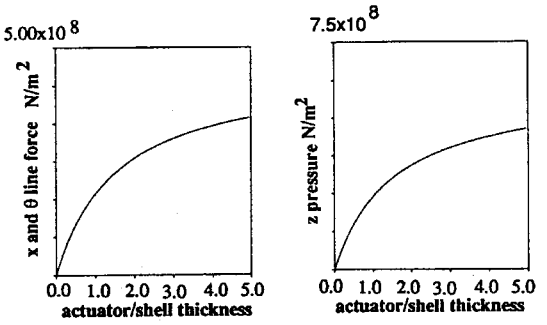

Fig. 9 Equivalent forces as functions of actuator thickness variation.

the extent of the actuator boundaries on the cylindrical shell surface. Substituting Eq. (27) for the free strains in the forcing terms of Eqs. (26) a true mathematical representation of the equivalent force can be obtained. Assuming that the free strains are also constant over the patch, then the differentiations involved in the forcing terms apply only to the Heaviside functions. After the substitution and the differentiations, the forcing terms F_x, F_θ, and F_z look as follows:

$$F_x = \bar{M}_{x1}[\delta(x-x_1) - \delta(x-x_2)][H(\theta-\theta_1) - H(\theta-\theta_2)]$$

$$F_\theta = \bar{M}_{\theta 1}[H(x-x_1) - H(x-x_2)][\delta(\theta-\theta_1) - \delta(\theta-\theta_2)] \quad (28)$$

$$F_z = \bar{M}_{z3}[H(x-x_1) - H(x-x_2)][H(\theta-\theta_1) - H(\theta-\theta_2)]$$

where $H(x)$ and $\delta(x)$ are the Heaviside function and Dirac's delta function. All of the equivalent forces have pressure units (newton per square meter) because all terms in all three dynamic equations are forces exerted per unit area. The equivalent force F_x (Fig. 7b) arises because of the variation of the force resultant N_{xx} (newton per meter) along the x coordinate and since $\delta(x)$ has 1/length units F_x is in newton per square meter. Because of the delta function along the x and the step function along the θ, it is confined to a line along the actuator boundary in the θ direction and, thus, is a line force. Similarly, F_θ (Fig. 7c) arises from the force resultant $N_{\theta\theta}$ and so is an in-plane line force in the θ direction. It should be easy to see that F_z is a uniform transverse pressure that arises due to the curvature effect on the in-plane normal θ force resultant.

Amplitude Variation of Equivalent Forces with Actuator Thickness

In this section the amplitude variation of the defined equivalent forces as a function of the actuator thickness is presented. Since the response of cylindrical shells to these forces varies considerably from one force to another, an insight into the dominant equivalent force as a function of the actuator thickness will help to tailor the actuator to achieve the desired cylindrical shell response.

Figure 9 shows the variation of each of the equivalent forces, namely, F_x, F_θ, and F_z as a function of the variation of the actuator thickness. The actuator thickness is varied from 0 to 5 times the shell thickness (actuator/shell thickness ratio = 5). The line forces keep increasing with the actuator thickness and level off after a certain value. This happens because the piezoactuator force proportional to the cross-sectional area of the actuator increases linearly with thickness. The same is true of the composite membrane stiffness and, thus, the ratio shows a saturating behavior. The behavior of the pressure force is a direct consequence of the θ line force behavior. The significance of this saturation value may be understood by looking at expression for F_θ in Eq. (26). It may be seen that this equation is symmetric with respect to Young's moduli, thicknesses of the shell, and the piezoactuators. Symmetry here implies that the variables (Y_s and Y_{pe} or h_1 and h_2) may be interchanged without changing the full expression. The distinction between shell and actuator is lost. This property is obtained because of the equivalent modulus approach used in the derivation whereby the individual membrane stiffnesses have been added to obtain the composite membrane stiffness. This is a valid approach provided the frequencies are such that the structural wavelengths are much larger than the shell/actuator thicknesses. Thus, as the thickness of the piezoelectric is increased without limit, its membrane stiffness begins to dominate and its properties cancel out from the numerator and denominator. The situation is analogous to a shell that has been bonded to a very stiff piezoelectric material. The final value of the expression is the force experienced by the shell material had it been the actuator and fully clamped (due to the infinitely stiff piezoelectric material).

Conclusions

In this investigation, a composite differential equation of motion for the curved piezoactuators and shell system was derived, and approximate analytical expressions for the equivalent forces exerted by the actuator on the shell were obtained. Transverse shear stresses were neglected based on previous flat actuator results, and also edge effects were assumed negligible for most of the actuator patch because of the small thickness. The in-phase configuration was studied. The piezoactuators exert x and θ line forces and a uniform pressure load over the patch for in-phase configuration. The in-phase forces show a saturation behavior with increase in thickness.

References

[1]Bailey, T., and Hubbard, J. E., "Distributed Piezoelectric-Polymer Active Vibration Control of a Cantilever Beam," *Journal of Guidance, Control, and Dynamics*, Vol. 8, No. 5, 1985, pp. 605–611.

[2]Baz, A., and Poh, S., "Optimum Vibration Control of Flexible Beams by Piezoelectric Ceramics," NASA CR-180209, 1987.

[3]Dimitriadis, E. K., Fuller, C. R., and Rogers, C. A., "Piezoelectric Actuators for Distributed Excitation of Thin Plates," *Journal of Vibration and Acoustics*, Vol. 113, Jan. 1991, pp. 100–107.

[4]Lee, C. K., "Piezoelectric Laminates for Torsional and Bending Modal Control: Theory and Experiment," Ph.D. Thesis, Dept. of Mechanical Engineering, Cornell Univ., Ithaca, NY, May 1987.

[5]Fuller, C. R., Snyder, S., Hansen, C., and Silcox, R., "Active Control of Interior Noise in Model Aircraft Fuselages using Piezoceramic Actuators," *AIAA 13th Aeroacoustics Conference* (Tallahassee, FL), AIAA, Washington, DC, 1990 (AIAA Paper 90-3922).

[6]Lester, H. C., and Lefebvre, S., "Piezoelectric Actuator Models for Active Sound and Vibration Control of Cylinders," *Proceedings of Recent Advances in Active Noise and Vibration Control* (Blacksburg, VA), Virginia Polytechnic Inst. and State Univ., Blacksburg, VA, 1991, pp. 3–26.

[7]Lester, H. C., and Silcox, R. J., "Active Control of Interior Noise in a Large Scale Cylinder using Piezoceramic Actuators," International Technical Specialists Meeting, Rotorcraft Acoustics and Rotor Fluid Dynamics, Philadelphia, PA, Oct. 1991.

[8]Silcox, R. J., Lefebvre, S., Metcalf, V. L., Beyer, T. B., and Fuller, C. R., "Evaluation of Piezoceramic Actuators for Control of Aircraft Interior Noise," DGLR/AIAA 14th Aeroacoustics Conf., Aachen, Germany, May 1992 (AIAA Paper 92-0291).

[9]Masters, A. A., Kim, S. J., and Jones, J. D., "Experimental Investigation into Active Control of Compressor Noise Radiation using Piezoelectric Actuators," *Inter-Noise 92* (Toronto, Canada), International Inst. for Noise Control, 1992, pp. 395–400.

[10]Sonti, V. R., and Jones, J. D., "Dynamic Effects of Mass and Stiffness of Piezoactuators on the Cylindrical Shell Response," *AIAA Journal* (to be published).

[11]Chaudhry, Z., Lalande, F., and Rogers, C. A., "Special Considerations in Modeling of Induced Strain Actuator Patches Bonded to Shell Structures," *Proceedings of the SPIE North American Conference on Smart Structures and Materials* (Orlando, FL), Feb. 1994, pp. 563–570.

[12]Soedel, W., *Vibrations of Plates and Shells*, Marcel Dekker, New York, 1981, p. 90.

[13]Fahy, F. J., *Sound and Structural Vibration: Radiation, Transmission and Response*, Academic, New York, 1985, p. 22.

[14]Boley, B. A., and Weiner, J. H., *Theory of Thermal Stresses*, Wiley, New York, 1960, pp. 356, 360.

[15]Crawley, E. F., and de Luis, J., "Use of Piezoelectric Actuators as Elements of Intelligent Structures," *AIAA Journal*, Vol. 25, No. 10, 1987, pp. 1373–1384.

[16]Seyoung, I., and Atluri, S. N., "Effects of a Piezo-Actuator on a Finitely Deformed Beam Subjected to General Loading," *AIAA Journal*, Vol. 27, No. 12, 1989, pp. 1801–1807.

[17]Kim, S. J., and Jones, J. D., "Optimal Design of Piezo-Actuators for Active Noise and Vibration Control," *AIAA Journal*, Vol. 29, No. 12, 1991, pp. 2047–2053.

[18]Liang, C., and Rogers, C. A., "Behavior of Shape Memory Alloy Actuators Embedded in Composites," *Proceedings of 1989 International Composites Conf.*, Beijing, PRC, Aug. 1989.